Pharmaceutical Research, Vol. 23, No. 6, June 2006 (© 2006)
DOI: 10.1007/s11095-006-0162-4

Research Paper

Oral Absorption of Poorly Water-Soluble Drugs: Computer Simulation of Fraction Absorbed in Humans from a Miniscale Dissolution Test

Ryusuke Takano,[1,4] Kiyohiko Sugano,[1,3] Atsuko Higashida,[1] Yoshiki Hayashi,[1] Minoru Machida,[1] Yoshinori Aso,[1] and Shinji Yamashita[2]

Received September 9, 2005; accepted January 31, 2006

Purpose. The purpose of this study was to develop a new system for computer simulation to predict fraction absorbed (F_a) of Biopharmaceutical Classification System (BCS) class II (low solubility–high permeability) drugs after oral administration to humans, from a miniscale dissolution test.
Methods. Human oral absorption of 12 lipophilic drugs was simulated theoretically by using the dissolution and permeation parameters of the drugs. A miniscale dissolution test and a solubility study were carried out in a conventional buffer and a biorelevant medium (pH 6.5). A dissolution parameter, which can simulate *in vivo* dissolution, was obtained from the *in vitro* dissolution curve. Human intestinal permeability was estimated assuming that the permeation was limited by diffusion through the unstirred water layer. The F_a in humans was predicted and then compared with clinical data.
Results. The dissolution and solubility of most model drugs were faster and higher in a biorelevant medium than in a conventional buffer. The simulated absorption was limited by the drug dissolution rate and/or solubility. Predicted F_a was significantly correlated with clinical data (correlation coefficient $r^2 = 0.82$, $p < 0.001$) when the dissolution profiles in biorelevant medium were used for the simulation.
Conclusions. This new system quantitatively simulated human absorption and would be beneficial for the prediction of human F_a values for BCS class II drugs.

KEY WORDS: computer simulation; dissolution; *in vitro–in vivo* correlation; oral absorption; poorly water-soluble.

INTRODUCTION

The drug discovery process has progressed through several technologies such as combinatorial chemistry and high-throughput *in vitro* pharmacology screening. As a result, drug candidates tend to have a large molecular weight, high hydrophobicity, and many hydrogen bonds (1). Such physicochemical properties often cause low solubility in water and may result in poor and variable oral absorption. To increase the probability of success in the subsequent development of compounds as an oral drug, prediction of human oral absorption for structurally diverse drugs is required for candidate selection at the early stage of drug discovery.

In the past, whole-animal studies were often carried out to determine oral absorption of new drug candidates. The combined effects of the factors that determine oral drug absorption, such as drug dissolution, membrane permeation, metabolism at the gut wall and liver, and gastrointestinal (GI) transit time, can be concurrently assessed in animal models. However, interspecies differences due to varying physiological conditions of the GI tract in oral absorption were often large for poorly water-soluble drugs. This may result in difficulty in predicting oral absorption in humans. In addition, the consumption of large amounts of compounds may not be suitable for drug discovery. Therefore, demand for *in vitro* screening tools that are able to predict human oral absorption in place of *in vivo* studies has increased.

Oral absorption from a solid dosage is determined by the dissolution rate, solubility, and intestinal membrane permeability (2). Theoretical computer models of dissolution and permeation processes in the GI tract have been developed to simulate oral absorption (3–5). However, in terms of the prediction of poorly water-soluble drugs, these models are insufficient because the physiological condition in the human GI tract, such as bile salts and food, are not reflected.

For Biopharmaceutical Classification System (BCS) class II drugs (low-solubility–high-permeability drugs, as defined by the Food and Drug Administration), dissolution rate and solubility are the principal limitations to absorption, and therefore these parameters should be key factors for predicting precise human absorption. The dissolution of these compounds depends on a variety of factors in the medium such as pH, surfactant, buffer capacity, and ionic strength. However, few reports are available on dissolution tests that

[1] Pre-clinical Research Department, Chugai Pharmaceutical Co. Ltd., 1-135 Komakado, Gotemba, Shizuoka, 412-8513, Japan.
[2] Faculty of Pharmaceutical Sciences, Setsunan University, 45-1 Nagaotoge-cho, Hirakata, Osaka, 573-0101, Japan.
[3] Present Address: Global Research & Development, Nagoya Laboratories, Pharmaceutical Sciences, Science & Technology, Pharmaceutical R&D, Pfizer Inc, 5-2 Taketoyo, Aichi, 470-2393, Japan.
[4] To whom correspondence should be addressed. (e-mail: takanorus@chugai-pharm.co.jp)

simulate quantitative *in vivo* dissolution in the human GI tract. Dissolution tests are usually used to ensure batch quality and to estimate bioequivalence or rank order of different formulations of a specific drug. Quantitative simulation of *in vivo* dissolution for structurally diverse drugs would be beneficial for evaluation of the absorbability of a drug substance.

To predict quantitative human oral absorption of structurally diverse BCS class II drugs at the candidate selection stage in drug discovery, we developed a new integrated system of a miniscale dissolution test with computer simulation. The predicted absorption of 12 model drugs was compared with clinical data to confirm the *in vitro–in vivo* correlation.

THEORY

Human oral absorption of poorly water-soluble drugs was simulated theoretically by using their dissolution and permeation parameters. A dissolution parameter, which can simulate the *in vivo* conditions, was extracted from an *in vitro* dissolution curve. Human intestinal permeability was estimated assuming that the permeation of those drugs was limited by diffusion through the unstirred water layer (UWL). Clinical oral absorption data of model drugs were collected from the literature to confirm the *in vitro–in vivo* correlation.

Extraction of Dissolution Parameter *z* from *in Vitro* Dissolution Curve

The Noyes-Whitney model was used to describe the dissolution of solid drugs (6). The model is based on the assumptions that drug particles are spheres of the same size, the surface area in a particle changes with time, and the ratio of D/h, where D is the diffusion coefficient and h is the diffusion layer thickness, is constant during the dissolution process. Drug weight is proportional to the number of particles based on the assumption of uniform particle size; therefore, the initial mass of solid drug ($X_{0,vitro}$) is a function of the number of the particles. The dissolution rate is given by the following equation:

$$\frac{dX_{d,vitro}(t)}{dt} = \frac{3D}{\rho h r_0} \times X_{o,vitro}\left(\frac{X_{s,vitro}(t)}{X_{o,vitro}}\right)^{2/3}\left(C_s - \frac{X_{d,vitro}(t)}{V_{vitro}}\right) = zX_{o,vitro}\left(\frac{X_{s,vitro}(t)}{X_{o,vitro}}\right)^{2/3}\left(C_s - \frac{X_{d,vitro}(t)}{V_{vitro}}\right) \quad (1)$$

where $X_{d,vitro}(t)$ is the mass of dissolved drug at time t, ρ is the density of the drug, r_0 is the initial particle radius, $X_{s,vitro}(t)$ is the mass of solid drug at time t, C_s is the saturated solubility of the drug, and V_{vitro} is the volume of the dissolution medium. z is the dissolution parameter, which is independent of the saturated solubility, applied amount of drug, and the volume of medium. The value of z is determined as $3D/\rho h r_0$, a hybrid parameter of the particle size, the diffusion coefficient, density of the drug, and the diffusion layer thickness. The z values were estimated from *in vitro* data using Eq. (1) with the mathematical software SAAM II version 1.2 (SAAM Institute Inc., University of Washington, Seattle, WA, USA).

Calculation of Unstirred Water Layer Permeability

Diffusion through the *UWL*, which is adjacent to the intestinal epithelial membrane, limits the intestinal permeation of highly permeable drugs. Because *UWL* permeation can be modeled as a simple diffusion process in a water layer, *UWL* permeability (P_{UWL}) is represented by the diffusion coefficient and the thickness (δ) of the *UWL* (7). The diffusion coefficient was assumed to follow the Stokes-Einstein equation for small, spherical molecules:

$$P_{UWL} = \frac{D}{\delta} = \frac{k_B T}{6\pi\eta\delta} \times \frac{1}{R} \quad (2)$$

where k_B is the Boltzmann constant, 1.38×10^{-23} J/K, T is the temperature in kelvin, η is the viscosity of the *UWL*, and R is the molecular radius. The effective intestinal membrane permeability (P_{eff}) of glucose in humans, the permeation of which is rate limited by the *UWL*, has been reported as 10×10^{-4} cm/s (8). R of glucose calculated by the McGowan volume (9) is 3.6 Å. Assuming that the permeation of glucose across the human intestine is completely limited by diffusion through the *UWL*, the diffusion layer thickness of *UWL* is expressed by the following equation. It has been calculated that the diffusion layer thickness (δ) of *UWL* is 100 μm (8,10) when the viscosity of water (0.653 mPa s at 313 K) (11) is used as *UWL* viscosity.

$$\delta = \frac{k_B T}{6\pi\eta} \times \frac{1}{R} \times \frac{1}{P_{UWL}} = \frac{k_B T}{6\pi\eta} \times \frac{1}{3.6} \times \frac{1}{10 \times 10^{-4}} \quad (3)$$

Then, $(P_{UWL})_R$ of each drug is given by substituting Eq. (3) into Eq. (2).

$$(P_{UWL})_R = 10 \times 10^{-4} \times \left(\frac{3.6}{R}\right) \quad (4)$$

The $(P_{UWL})_R$ is the *UWL* permeability calculated with the molecular radius of the drug. Molecular radius is a function of the cube root of the molecular weight, $(MW)^{1/3}$, assuming a spherical molecule, and so the diffusion layer thickness can also be expressed using *MW*. The *MW* of glucose is 180.

$$\delta = \frac{k_B T}{6\pi\eta} \times \frac{1}{\left(\frac{3}{4\pi\rho} \times MW\right)^{1/3}} \times \frac{1}{P_{UWL}} = \frac{k_B T}{6\pi\eta} \times \frac{1}{\left(\frac{3}{4\pi\rho} \times 180\right)^{1/3}} \times \frac{1}{10 \times 10^{-4}} \quad (5)$$

The $(P_{UWL})_{MW}$ for each drug is given by substituting Eq. (5) into Eq. (2). The $(P_{UWL})_{MW}$ is the *UWL* permeability of each drug calculated with the molecular weight of the drug. *MW* is simpler to obtain than molecular radius.

$$(P_{UWL})_{MW} = 10 \times 10^{-4} \times \left(\frac{180}{MW}\right)^{1/3} \quad (6)$$

Simulation of Absorption in the Small Intestine

The model accounting for the dissolution and the passive permeation of a drug in the small intestine assumes (i) the drug dissolves in the small intestine, not in the stomach and colon; (ii) the diffusion layer models the dissolution process [Eq. (7)]; (iii) the drug absorbs in the small intestine, not in the stomach or colon; (iv) membrane permeability of a lipophilic drug is high enough to be limited by diffusion through the *UWL*; (v) 4 h of transit time in the small intestine (12); and (vi) literature values of the effective intestinal surface area S (800 cm^2) and the small intestinal fluid volume V_{vivo} (600 mL) are correct (4,13,14). Mass balances of solid and dissolved drugs in the GI tract are given by:

$$\frac{dX_{s,vivo}(t)}{dt} = -zX_{0,vivo}\left(\frac{X_{s,vivo}(t)}{X_{0,vivo}}\right)^{2/3}\left(C_s - \frac{X_{d,vivo}(t)}{V_{vivo}}\right) \quad (7)$$

$$\frac{dX_{d,vivo}(t)}{dt} = zX_{0,vivo}\left(\frac{X_{s,vivo}(t)}{X_{0,vivo}}\right)^{2/3}\left(C_s - \frac{X_{d,vivo}(t)}{V_{vivo}}\right) - (P_{UWL})_{MW} \times S \times \frac{X_{d,vivo}(t)}{V_{vivo}} \quad (8)$$

where $X_{s,vivo}(t)$ is the mass of solid drug in the small intestine at time t and $X_{d,vivo}(t)$ is the mass of dissolved drug in the small intestine at time t. $X_{0,vivo}$, which is the function of the number of particles *in vivo*, was set equal to a clinical dose. z and C_s obtained from *in vitro* tests were used. The rate of absorption is given by:

$$\frac{dX_{a,vivo}(t)}{dt} = (P_{UWL})_{MW} \times S \times \frac{X_{d,vivo}(t)}{V_{vivo}} \quad (9)$$

where $X_{a,vivo}(t)$ is the mass of absorbed drug at time t. The total mass of dissolved drug at time t, $X_{d,total}(t)$, is given by the difference between clinical dose (initial mass of solid drug) and the mass of solid drug.

$$X_{d,total}(t) = X_{0,vivo} - X_{s,vivo}(t) \quad (10)$$

$C_{ratio}(t)$ is the ratio of the intestinal drug concentration at time t against the drug saturated solubility, shown here as a percentage.

$$C_{ratio}(t)(\%) = \frac{X_{d,vivo}(t)/V_{vivo}}{C_s} \times 100 \quad (11)$$

The concentration gradient across the diffusion layer of solid surface h, which represents $[C_s - (X_{d,vivo}(t)/V_{vivo})]/h$, controls dissolution at a time point. If the $C_{ratio}(t)$ is low ($C_s \gg X_{d,vivo}(t)/V_{vivo}$), the drug dissolves under sink conditions. If the $C_{ratio}(t)$ increases, drug dissolution decreases due to the limitation of its solubility (nonsink conditions).

The predicted fraction absorbed (F_a) is the ratio between $X_{0,vivo}$ and $X_{a,vivo}(t)$ at the time of 4 h.

$$F_a(\%) = \frac{X_{a,vivo}(t)}{X_{0,vivo}} \times 100 \quad (12)$$

To obtain simulated profiles, the Runge-Kutta method was used in STELLA®5.1.1 software (Cognitus Ltd., North Yorkshire, UK).

Drug Selection

For the models of poorly water-soluble drugs, neutral, free weak acid, and free weak base drugs were selected. Their oral absorption largely depends on dissolution in the small intestine based on the following: (a) neutral drugs mainly dissolve in the small intestine but not in the stomach and colon because of the presence of bile salts and (b) free weak acids also mainly dissolve in the small intestine but not in the stomach and colon because of high pH and the presence of bile salts. In the case of free weak bases, they usually dissolve in the stomach due to low gastric pH; however, (c) when the gastric pH is elevated (achlorhydria, the patients receiving gastric acid blockers and some pathological conditions), they will dissolve not in the stomach but mainly in the small intestine because of the presence of bile salts. Therefore, free weak base drugs were used in this study when the clinical absorption data in the subject having elevated gastric pH were available.

Collection of Clinical Oral Absorption Data

The value of fraction absorbed in humans was needed to confirm the predictability of the present system. However, only a few reports have been published on the human F_a of BCS class II drugs. The present study utilized clinical absorption data, serving as an alternative to F_a. The clinical data of the drugs collected from the literature are listed and referenced in Table VI.

Fraction of Dose Absorbed

Oral bioavailability (BA) of a drug is a function of F_a, the fraction of the dose-escaping metabolism by the GI mucosa (F_g) and by the liver (F_h).

$$BA = F_a \times F_g \times F_h \quad (13)$$

F_a of dipyridamole and gefitinib were calculated from their BA in the fasted state and F_h assuming that hepatic clearance is the only elimination pathway. F_h was estimated using total plasma clearance after intravenous administration in humans. Total plasma clearance of dipyridamole (15) and gefitinib [approval documentation for Iressa® (gefitinib) in Japan, AstraZeneca, Osaka, Japan, 2002) was reported to be 138 and 514 mL/min, respectively. The hepatic blood flow value of 1400 mL/min is from literature data (16).

Relative Bioavailability of a Solid Dosage Form and a Solution Orally Administered in the Fasted States

The relative BA was calculated as the ratio of the area under the curve for solid dosages (AUC_{solid}) to solution dosages ($AUC_{solution}$), or *rel.* $BA_{solid/solution}$, where AUC_{solid} is

the product of $F_{a,solid}$, $F_{g,solid}$, and $F_{h,solid}$ and $AUC_{solution}$ is the product of $F_{a,solution}$, $F_{g,solution}$, and $F_{h,solution}$

$$rel.BA_{solid/solution} = \frac{AUC_{solid}}{AUC_{solution}} = \frac{F_{a,solid} \times F_{g,solid} \times F_{h,solid}}{F_{a,solution} \times F_{g,solution} \times F_{h,solution}} \quad (14)$$

Assuming linear kinetics of drug metabolism in both administrations, the relative bioavailability represents the ratio of $F_{a,solid}$ and $F_{a,solution}$. Lipophilic drugs administered as a solution could be completely absorbed due to their high permeability. Therefore, the rel. $BA_{solid/solution}$ is almost equal to $F_{a,solid}$ in the fasted state.

Relative Bioavailability of a Solid Dosage Form Orally Administered in the Fasted and Fed States

The relative BA was calculated as the ratio of the area under the curve for solid dosages in the fasted (AUC_{fasted}) to fed states (AUC_{fed}), or *rel.* $BA_{fasted/fed}$, where AUC_{fasted} is the product of $F_{a,fasted}$, $F_{g,fasted}$, and $F_{h,fasted}$ and AUC_{fed} is the product of $F_{a,fed}$, $F_{g,fed}$, and $F_{h,fed}$.

$$rel.BA_{fasted/fed} = \frac{AUC_{fasted}}{AUC_{fed}} = \frac{F_{a,fasted} \times F_{g,fasted} \times F_{h,fasted}}{F_{a,fed} \times F_{g,fed} \times F_{h,fed}} \quad (15)$$

Intestinal bile levels are much higher in the fed than in the fasted state (17,18). Because the greater concentrations of bile salts and lecithin can enhance the solubility of lipophilic drugs (19), almost complete absorption may occur in the fed state. Therefore, the *rel.* $BA_{fasted/fed}$ of these drugs can be regarded roughly as the F_a of a solid dosage form in the fasted state, assuming high permeability to the intestinal wall and linear kinetics of metabolism.

Oral Absorption of Free Weak Base Drugs in Subjects with Elevated Gastric pH

Subjects who were given gastric acid blockers usually had a high gastric pH of around 6.0 or higher (20). The oral absorption of dipyridamole, gefitinib, and ketoconazole in subjects with elevated gastric pH treated with gastric acid blockers is significantly lower than that of subjects with low gastric pH (20,21) [approval documentation for Iressa® (gefitinib) in Japan, AstraZeneca, Osaka, Japan, 2002]. Dipyridamole, gefitinib, and ketoconazole are weak bases with pK_a values of 5.7, 4.7, and 6.5, respectively (Table I). The saturated solubility of these drugs at pH values ranging from 4.0 to 6.5 was studied and found to decrease by almost two orders of magnitude from pH 4.0 to 6.0 (data not shown). These observations suggest that their oral absorption in high gastric pH subjects largely depends on dissolution in the small intestine but not in the stomach because of the presence of bile salts. The F_a in subjects with elevated gastric pH ($F_{a,high}$) is obtained from the F_a in subjects with low gastric pH ($F_{a,low}$) and the relative bioavailability of subjects with high gastric pH against low gastric pH (*rel.* $BA_{high/low}$).

$$F_{a,high} = F_{a,low} \times rel.BA_{high/low} \quad (16)$$

$F_{a,low}$ of dipyridamole and gefitinib were calculated from their BA and F_h [Eq. (13)]. The *rel.* $BA_{solid/solution}$ as $F_{a,low}$ of

Table I. Drug Properties and Formulation Products Used in this Study

Drug name	Ionization properties	MW	log D (6.5)[a]	Product name
Danazol	Neutral	337.5	4.0	Bonzol® tablets (Mitsubishi Pharma Corporation, Osaka, Japan)
Dipyridamole	pK_a[b] = 5.7, 12.5; both alkaline	504.6	1.7	Anginal® tablets (Yamanouchi Pharmaceutical Co., Ltd., Tokyo, Japan)
Efavirenz	Neutral	315.7	4.1	Stocrin® capsules (Banyu Pharmaceutical Co., Ltd., Tokyo, Japan)
Exemestane	Neutral	296.4	4.1	Aromasin® tablets (Pfizer Japan Inc., Tokyo, Japan)
Gefitinib	pK_a[a] = 4.7, 7.6; both alkaline	446.9	2.9	Iressa® tablets (AstraZeneca K.K., Tokyo, Japan)
Griseofulvin	Neutral	352.8	2.9	Guservin FP® tablets (Chugai Pharmaceutical Co., Ltd., Tokyo, Japan)
Ivermectin	Neutral	875.1	6.5	Stromectol® tablets (Banyu Pharmaceutical Co., Ltd., Tokyo, Japan)
Ketoconazole	pK_a[c] = 2.9, 6.5; both alkaline	531.4	3.2	Nizoral® tablets (Janssen Pharmaceutical Products, LP, Titusville, NJ, USA)
Ketoprofen	pK_a[d] = 4.6; acidic	254.3	0.7	Capisten® capsules (Kissei Pharmaceutical Co., Ltd., Matsumoto, Japan)
Nitrendipine	Neutral	360.4	3.3	Baylotensin® tablets (Mitsubishi Pharma Corporation, Japan)
Phenytoin	pK_a[e] = 8.3; acidic	252.3	1.6	Aleviatin® tablets (Dainippon Pharmaceutical Co., Ltd., Osaka, Japan)
Spironolactone	Neutral	416.6	3.3	Aldactone-A® tablets (Pfizer Japan Inc.)

[a] Calculated by Pallas 3.1.
[b] Ref. (42).
[c] Ref. (43).
[d] Ref. (44).
[e] Ref. (45).

Table II. HPLC Conditions used to Determine the Concentration of each Drug

Drug name	Wavelength (nm)	Mobile phase composition (A:B)
Danazol	284	30:70
Dipyridamole	270	70:30
Efavirenz	240	40:60
Exemestane	245	50:50
Gefitinib	250	75:25
Griseofulvin	320	55:45
Ivermectin	240	15:85
Ketoconazole	270	70:30
Ketoprofen	235	55:45
Nitrendipine	254	45:55
Phenytoin	205	65:35
Spironolactone	245	50:50

Column temperature and flow rate were 40°C and 1.0 mL/min, respectively. Mobile phase A was water with 0.1% trifluoroacetic acid. Mobile phase B was acetonitrile with 0.1% trifluoroacetic acid.

ketoconazole was calculated from the *AUCs* of solid and solution dosage form administrations [Eq. (14)] (22).

MATERIALS AND METHODS

Materials

Commercially available formulation products of the drugs tested in this study are listed in Table I. The log *D* values of these drugs and the pK_a values of gefitinib were calculated from the chemical structures of the drugs using Pallas 3.1 software (CompuDrug, Hungary).

Danazol, dipyridamole, exemestane, griseofulvin, ivermectin, ketoconazole, spironolactone, ketoprofen, and Lucifer yellow were purchased from Sigma Chemical (St. Louis, MO, USA). Phenytoin, nitrendipine, and sodium taurocholate were purchased from Wako Pure Chemical Industries (Osaka, Japan). L-α-Phosphatidylcholine was purchased from Nippon Oil and Fats Corporation (Tokyo, Japan). Efavirenz (23) and gefitinib (24) were isolated from Stocrin® capsules and Iressa® tablets, respectively.

The 0.45-μm polyvinylidene fluoride membrane filter was purchased from Millipore Corporation (Billerica, MA, USA).

Miniscale Dissolution Tests

Dissolution tests were carried out using a VK7010 dissolution station and a VK8000 dissolution sampling station with a 100-mL conversion kit (Vankel Technologies, Inc., Cary, NC, USA). The kit consists of a 100-mL glass vessel (42 mm diameter × 105 mm) and a Teflon-coated minipaddle (29.8-mm-diameter paddle with a 63.5-mm shaft). The dissolution tests were carried out for 4 h in 50 mL of medium at 37°C with a paddle speed of 50 rpm. The paddle distance from the vessel bottom was 1.0 cm. To circumvent the disintegration process of formulations, crushed tablets or the contents of capsules were added to the vessels. Experiments were run in triplicate. Samples (500 μL) were withdrawn at determined times and filtered through 0.45-μm filters. The first 10 mL was filtered and circulated through tubing to avoid loss of drug from the sample due to adsorption. The sample was diluted with the same volume of tetrahydrofuran.

Simulated intestinal fluid (SIF, pH 6.5) without bile salt was prepared according to Japanese Pharmacopoeia XIV. The pH adjustment was made using 1 M HCl. Fasted-state simulated intestinal fluid (FaSSIF) is a physiologically biorelevant medium containing 3 mM sodium taurocholate and 0.75 mM lecithin in a pH 6.5 phosphate buffer (25). This condition mimics the average conditions in the proximal human intestine in the fasted state.

Saturated Solubility Study

Saturated solubility was determined after 24 h equilibration in medium at a temperature of 37°C using a shaking

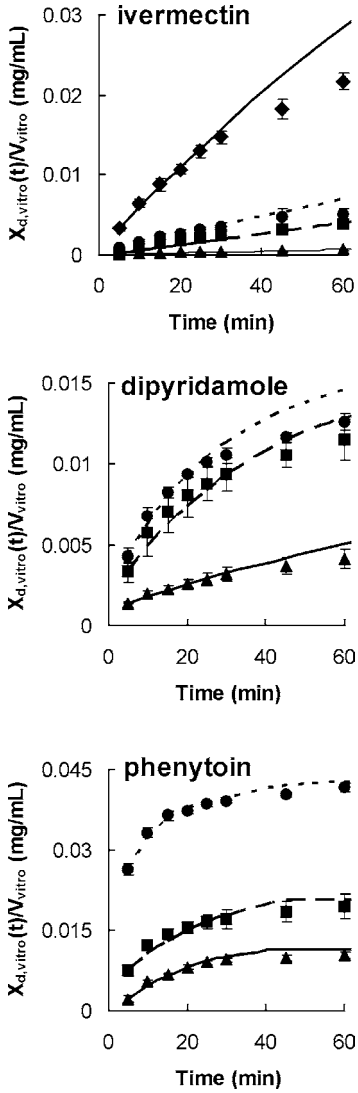

Fig. 1. Effect of applied amount on the dissolution of ivermectin, dipyridamole and phenytoin in FaSSIF. The mean concentration–time profiles and fitting curves of ivermectin at 0.2 mg (▲, —), 1.1 mg (■, - - -), 1.9 mg (●, ···), 9.0 mg (♦, —); dipyridamole at 1.3 mg (▲, —), 5.2 mg (■, - - -), 7.7 mg (●, ···); and phenytoin at 0.6 mg (▲, —), 1.2 mg (■, - - -), 5.1 mg (●, ···) (mean ± SD). Fitting curves were obtained assuming that the drugs dissolved according to the Noyes-Whitney theory.

Table III. The Dissolution Parameter z Obtained from the Dissolution Curve of Ivermectin, Dipyridamole, and Phenytoin at Various Applied Amounts (Mean ± SD)

Drug name	Applied amount $X_{0,vitro}$ (mg)	z (mL mg^{-1} min^{-1})
Ivermectin	0.2	0.029 ± 0.005
	1.1	0.028 ± 0.002
	1.9	0.026 ± 0.006
	9.0	0.026 ± 0.001
Dipyridamole	1.3	0.213 ± 0.035
	5.2	0.248 ± 0.045
	7.7	0.229 ± 0.015
Phenytoin	0.6	1.259 ± 0.083
	1.2	1.142 ± 0.172
	5.1	1.126 ± 0.060

water bath. Screw-capped amber glass vials containing 10 mL of medium were positioned in the water bath. Excess amounts of drugs in the formulations were then added to the vials. Experiments were carried out in triplicate. After 24 h, aqueous samples were filtered through 0.45-μm filters. The first 9 mL was discarded to avoid loss of drug from the sample due to adsorption. The remainder of the sample was diluted with the same volume of tetrahydrofuran.

High-Performance Liquid Chromatography Analysis

Sample concentrations of the dissolution test and the solubility study were determined by high-performance liquid chromatography (HPLC, Waters 2795 separation module, Waters, Milford, MA) using a UV detector (Waters 2487 dual λ UV/VIS detector, Waters). Diluted samples (10 μL) were injected into a C18 column (Cadenza CD-C18 3 μm 3.0 × 50 mm, Imtakt Corporation, Kyoto, Japan) and eluted with a mobile phase. The HPLC conditions used to determine the concentration of each drug are shown in Table II. A standard curve was prepared for each drug and linearity was observed at a concentration range of approximately 0.2–200 μg/mL on a log–log plot (correlation coefficient $r^2 > 0.999$) using linear regression analysis in Microsoft Excel 2000 (Microsoft,

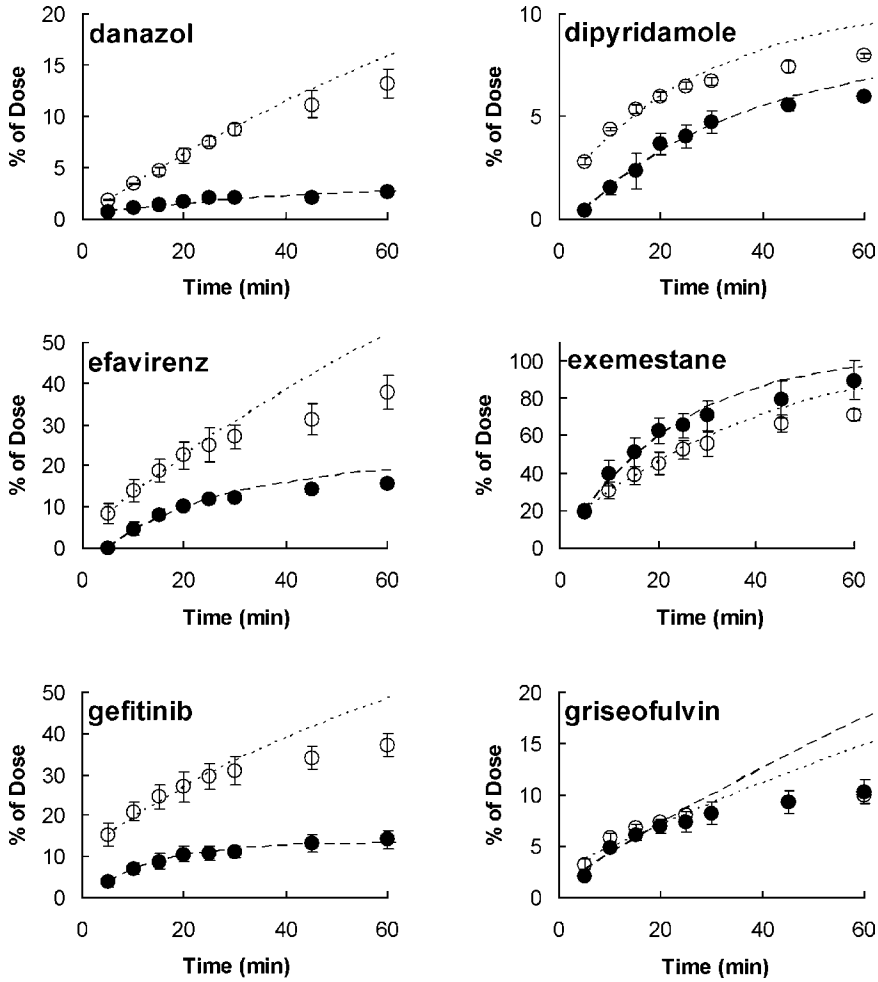

Fig. 2. Time profiles of cumulative percent dissolved and the fitting curves of BCS class II drugs in simulated intestinal buffer (pH 6.5) with 3 mM sodium taurocholate and 0.75 mM lecithin (FaSSIF, ○, ···) and without bile salt and lecithin (SIF, ●, - - -) (mean ± SD). Fitting curves were obtained assuming that the drugs dissolved according to the Noyes-Whitney theory.

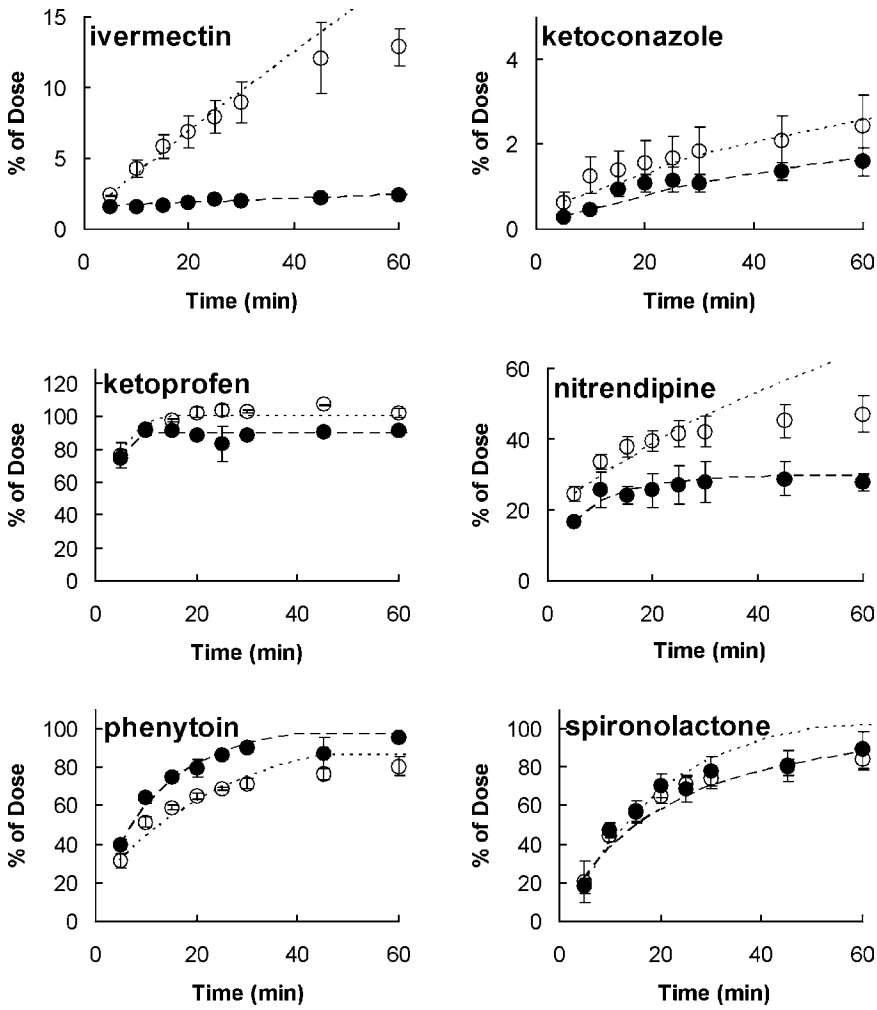

Fig. 2. Continued.

Redmond, WA). The accuracies of back-calculated concentrations were 94.0–107.9%.

Preparation of Caco-2 Monolayers

The Caco-2 cell line was obtained at passage 17 from American Type Culture Collection (Rockville, MD, USA). The cells were cultured in Dulbecco's modified Eagle's medium (DMEM) supplemented with 10% fetal bovine serum (FBS), 1% nonessential amino acids (NEAA), and 2 mM L-glutamine in a humidified incubator (5% CO_2, 37°C). The Caco-2 monolayer was prepared by using the Biocoat HTS Caco-2 Assay System (Becton Dickinson Bioscience, Bedford, MA, USA) with minor modifications. Briefly, before reaching full confluence, the cells were detached with 0.25% trypsin and 0.02% EDTA and removed from the culture flask. On day 0, the cells were plated at a density of 1.29×10^5 cells/cm^2 in DMEM supplemented with 0.5% FBS, 1% NEAA, and 2 mM L-glutamine on fibrillar collagen-coated inserts (1.0-μm pore, 0.31-cm^2 growth area). On day 3, the medium was replaced with Basal Seeding Medium containing MITO+™ Serum Extender, a concentrated lyophilized formulation of hormones, growth factors, and metabolites required for the maintenance of cells under serum-free conditions. Transport experiments were performed on day 7.

Permeation Experiments in Caco-2 Monolayers

The transport of each drug in the apical to basal direction was examined (apical medium: pH 6.0 containing 1% dimethyl sulfoxide and 4% dimethylacetamide; basal medium: pH 7.4 containing 4% bovine serum albumin). Dimethylacetamide was added to the apical medium as a solubilizer for the poorly water-soluble drugs (26). Hank's balanced salt solution (HBSS) containing 25 mM glucose was used. Prior to the experiments, the monolayer was washed twice with HBSS. Transport experiments were initiated by adding the medium containing the drugs listed in Table I. Lucifer yellow (0.5 mg/mL) was used as a paracellular marker compound to check the integrity of the monolayer during the incubation. The monolayer was incubated for up to 2 h at 37°C.

The samples were extracted by using a solid-phase extraction kit (Oasis μElution Plate® HLB, SPE cartridges, Waters). The concentration of the drugs in the apical and

basal compartments was determined by liquid chromatography/ mass spectrometry (LC/MS; micromass ZQ-alliance 2790 separation module, Waters) with a C18 column (Xterra MS-C18, 3.5 μm, 2.1 × 30 mm, Waters). The eluents consisted of H_2O/acetonitrile (MeCN)/trimethylamine in ratios of 100:0:0.6 (v/v, solvent A) and 0:100:0 (v/v, solvent B). Elution was accomplished by using a linear gradient that consisted of ramping from 3% to 100% B for 5 min. The ($1/\chi^2$) linear regression analysis showed correlation coefficients of linearity ($r^2 > 0.972$) at a concentration range of 0.2–10 μM. The accuracies of back-calculated concentrations were 75.2–122.9%. The concentration of ivermectin was quantified by HPLC (Waters 2795 separation module, Waters) using a UV detector (Waters 2487 dual λ UV/VIS detector, Waters) with a C18 column (Cadenza CD-C18, 3 μm, 3.0 × 50 mm, Imtakt, Japan). HPLC conditions are shown in Table II. The concentration of Lucifer yellow was determined with a microtiter plate reader (Spectramax 190, Molecular Devices, Sunnyvale, CA, USA) at excitation and emission wavelengths of 430 and 530 nm, respectively.

The apparent permeability coefficient (P_{app}) of each drug was calculated with the following equation:

$$P_{app} = \frac{dQ}{dt} \times \frac{1}{A \times C_0} \tag{17}$$

where dQ/dt is the flux of a drug across the monolayer (micromoles per second), A is the surface area of the monolayer (centimeters squared), and C_0 is the initial drug concentration on the apical side (millimoles per liter).

RESULTS

Miniscale Dissolution Test and Solubility Study

Figure 1 shows the dissolution profiles of the formulation products of ivermectin, dipyridamole, and phenytoin in FaSSIF at various applied amounts. The dissolution parameter z for each formulation was obtained from fitting the dissolution result to Eq. (1) (Table III). The z values for ivermectin, dipyridamole, and phenytoin were almost the same (not statistically significant) and independent of the applied amount because the apparent dissolution rate is also dose dependent.

The dissolution tests were carried out for the 12 lipophilic drugs (applied amount = 1 mg). The dissolution profiles and the fitting curves in SIF and FaSSIF are illustrated in Fig. 2. The formulation products of most of the drugs dissolved faster in FaSSIF than in SIF. The dissolution of exemestane and phenytoin was slightly faster in SIF than in FaSSIF.

The saturated solubility of each drug in SIF and FaSSIF was determined by the saturated solubility study (Table IV). The saturated solubility of the model drugs increased 1.1–160 times in FaSSIF compared to the solubility in SIF.

The z value of each drug was obtained from the dissolution curve in SIF and FaSSIF and is summarized in Table IV. Except for ketoprofen, the z values of tested drugs were smaller in FaSSIF than in SIF, suggesting that the diffusivity of drugs decreased in FaSSIF. In the case of ketoprofen, the z value did not change because the saturated solubility and dissolution were high and fast in both media.

Permeability Measurement and Calculation

P_{app} values of the 12 drugs were measured in Caco-2 monolayers (Table V). The permeability of Lucifer yellow was 6.5 ± 1.7 10^{-7} cm/s, confirming that the integrity of the Caco-2 monolayers was well maintained during the experiments. The permeability of model drugs to Caco-2 monolayers was more than 2.7 × 10^{-5} cm/s, except for ivermectin. Ivermectin was hardly detected on the basal side for 2 h although the concentration on the apical side decreased. Therefore, the permeability of ivermectin was not determined.

P_{UWL} values were calculated from human permeability of glucose by using Eqs. (4) and (5). The molecular radius and the cube root of the molecular weight of each drug were used as parameters. Figure 3 shows the relationship between the P_{UWL} values calculated with these parameters using unweighted least squares regression analysis. The $(P_{UWL})_{MW}$ values were almost the same as the $(P_{UWL})_R$ values (correlation coefficient $r^2 = 0.94$, t statistic $p < 0.001$, $n = 12$). Random error and the standard deviation of percent difference was 3.9 ± 1.8, which was estimated from percent

Table IV. The Dissolution Parameter and the Saturated Solubility of Twelve Drugs in SIF and FaSSIF (Mean ± SD)

	z (mL mg^{-1} min^{-1})		C_s (mg mL^{-1})	
Drug name	SIF	FaSSIF	SIF	FaSSIF
Danazol	0.307 ± 0.054	0.269 ± 0.023	0.002 ± 0.001	0.012 ± 0.001
Dipyridamole	0.442 ± 0.11	0.229 ± 0.015	0.006 ± 0	0.017 ± 0.002
Efavirenz	0.897 ± 0.187	0.053 ± 0.004	0.01 ± 0.001	0.194 ± 0.007
Exemestane	0.937 ± 0.273	0.411 ± 0.074	0.048 ± 0.002	0.061 ± 0.002
Gefitinib	0.738 ± 0.206	0.315 ± 0.028	0.009 ± 0.001	0.034 ± 0.006
Griseofulvin	0.284 ± 0.067	0.183 ± 0.033	0.016 ± 0	0.019 ± 0
Ivermectin	0.344 ± 0.036	0.026 ± 0.006	0.0007 ± 0	0.12 ± 0.01
Ketoconazole	0.028 ± 0.007	0.022 ± 0.006	0.012 ± 0	0.021 ± 0.001
Ketoprofen	0.065 ± 0.058	0.073 ± 0.005	2.249 ± 0.062	2.504 ± 0.078
Nitrendipine	2.319 ± 0.743	1.077 ± 0.092	0.004 ± 0.001	0.016 ± 0.002
Phenytoin	2.436 ± 0.378	1.142 ± 0.172	0.039 ± 0.002	0.043 ± 0.002
Spironolactone	1.945 ± 0.756	1.427 ± 0.163	0.03 ± 0	0.042 ± 0.002

Table V. P_{app} Determined from Caco-2 Monolayers (Mean ± SD)

Drug name	P_{app} ($\times 10^{-5}$ cm/s)
Danazol	8.73 ± 4.98 (n = 4)
Dipyridamole	2.70 ± 0.12 (n = 2)
Efavirenz	8.92 ± 6.77 (n = 2)
Exemestane	4.71 ± 0.49 (n = 4)
Gefitinib	3.29 ± 0.01 (n = 2)
Griseofulvin	5.83 ± 0.10 (n = 2)
Ivermectin[a]	–
Ketoconazole	6.56 ± 1.02 (n = 2)
Ketoprofen	5.96 ± 1.27 (n = 8)
Nitrendipine	10.14 ± 0.39 (n = 2)
Phenytoin	5.92 ± 0.96 (n = 2)
Spironolactone	4.91 ± 2.35 (n = 4)

[a] Ivermectin was not detected in the basal side although the concentration in the apical side decreased.

difference normalized to the $(P_{UWL})_R$. The 95% confidence intervals of intercept and slope were −0.00014 to 0.00014 and 0.79 to 1.15. Therefore, we used the value of $(P_{UWL})_{MW}$ for the simulation to simplify the calculations.

Oral Absorption Prediction

Intestinal absorption [the amount of the solid drug $X_{s,vivo}(t)$, the dissolved drug $X_{d,vivo}(t)$, and the absorbed drug $X_{a,vivo}(t)$] was simulated by Eqs. (7) – (9) using the saturated solubility and the z values in SIF and FaSSIF, UWL permeability, and clinical doses. Time-related profiles of the total amounts of the dissolved drugs $X_{d,total}(t)$, $X_{a,vivo}(t)$, and $C_{ratio}(t)$ (%) were obtained for all drugs. Figures 4 and 5 show the simulated results of ivermectin and efavirenz using the dissolution results in FaSSIF. The simulated amount of the absorbed drug, $X_{a,vivo}(t)$, was almost the same as the total amounts of the dissolved drug, $X_{d,total}(t)$, at any time point for both drugs. The C_{ratio}, which is the ratio of intestinal drug concentration and saturated solubility, of ivermectin was very low. On the other hand, the C_{ratio} of efavirenz was more than 40% within 4 h. The results indicate that ivermectin dissolves in the small intestine under sink condition and efavirenz dissolves under nonsink condition in the present simulation.

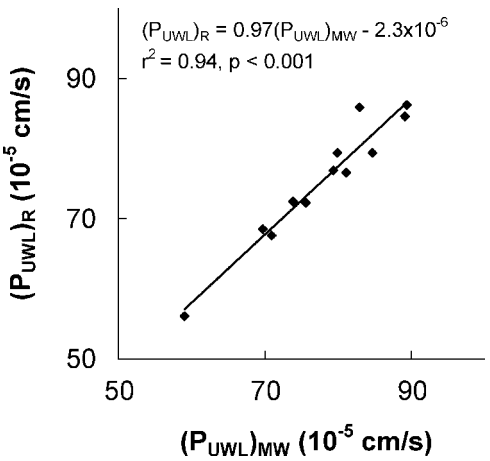

Fig. 3. Relationship between *UWL* permeability P_{UWL} (centimeters per second) of 12 model drugs calculated from the molecular radius $(P_{UWL})_R$ and from the cube root of molecular weight $(P_{UWL})_{MW}$.

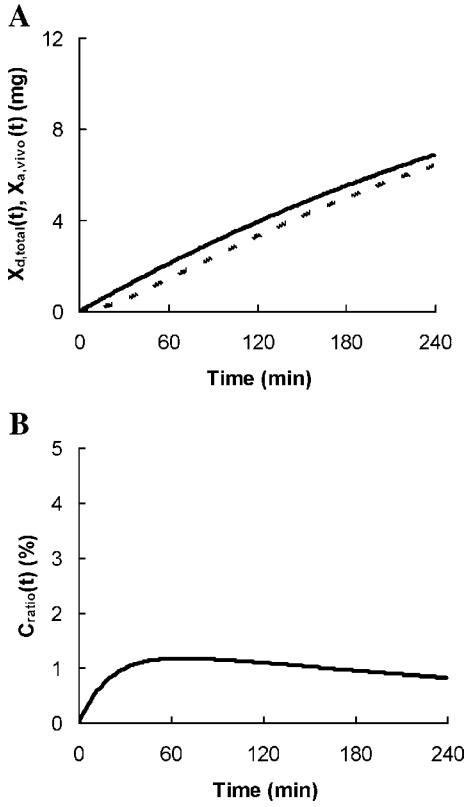

Fig. 4. (A) Time profiles of simulated total mass of the dissolved ivermectin in the small intestine, $X_{d,total}(t)$ (–), the simulated mass of the absorbed ivermectin, $X_{a,vivo}(t)$ (···), and (B) the simulated percentage of the intestinal ivermectin concentration against the saturated solubility, $C_{ratio}(t)$, using Eqs. (7) – (11) with the dissolution results in FaSSIF.

The F_a of each drug was calculated from the simulated absorption amount after 4 h and the clinical dose (Table VI). The prediction using SIF dissolution results gave smaller F_a values of most drugs compared to FaSSIF results. The absorption of exemestane, ketoprofen, phenytoin, and spironolactone was simulated to be complete by using the parameters from both SIF and FaSSIF. Figure 6 shows the relationship between predicted and observed F_a in humans when the dissolution results in FaSSIF were used for the simulation. The correlation coefficients (r^2) were 0.59 (SIF results) and 0.82 (FaSSIF results) using unweighted least squares regression analysis. The t statistic of the correlation coefficients showed $p < 0.001$, $n = 12$. The root mean squared error (RMSE), which is a predictability indicator (27), was 27% for the SIF results and 16% for the FaSSIF results.

$$RMSE = \sqrt{\frac{\sum_1^N (observed F_a - predicted F_a)^2}{N}} \quad (18)$$

DISCUSSION

Nicolaides *et al.* reported the plasma profiles of seven formulation products of four lipophilic drugs (28,29). They simulated drug dissolution *in vivo* from *in vitro* dissolution test data assuming a drug dissolves under sink condition.

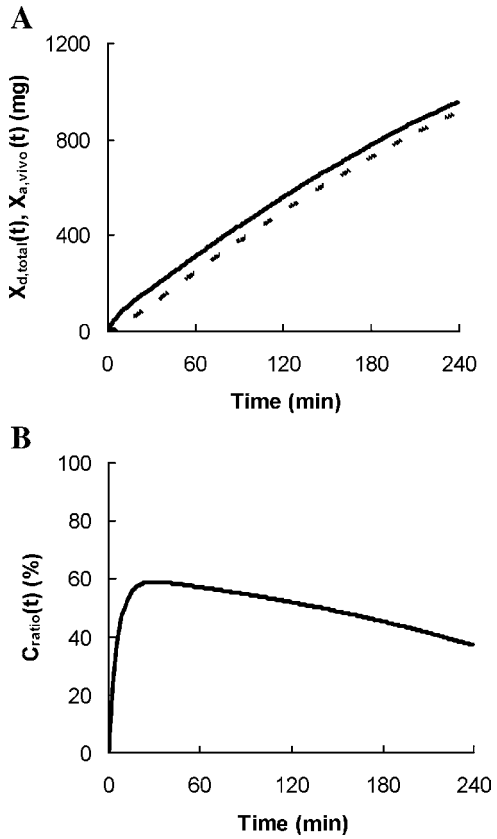

Fig. 5. (A) Time profiles of simulated total mass of the dissolved efavirenz in the small intestine, $X_{d,total}(t)$ (–), the simulated mass of the absorbed efavirenz, $X_{a,vivo}(t)$ (···), and (B) the simulated percentage of the intestinal efavirenz concentration against the saturated solubility, $C_{ratio}(t)$, using Eqs. (7) – (11) with the dissolution results in FaSSIF.

Their study is useful to evaluate oral absorption of drugs (from different formulation products) and the effects of food on a drug. However, they simulated only drug dissolution, not drug permeation, although both processes sequentially occur in oral absorption. Their system does not evaluate drug dissolution *in vivo* under nonsink dissolution. In addition, because newly synthesized compounds are often available only in limited amounts, a large-scale dissolution test (500 mL) is unacceptable for the drug discovery stage. In contrast, we have developed a new system integrating a miniscale dissolution test with computer simulation to quantitatively predict the amount of fraction absorbed of structurally diverse BCS class II drugs. This system, which simulates both the drug dissolution and the permeation process in the GI tract, could reflect drug dissolution under sink and nonsink conditions. The predictability of the fraction of drug absorbed was confirmed using 12 structurally diverse BCS class II drugs.

To simulate the drug dissolution *in vivo* from dissolution profile *in vitro*, in a miniscale dissolution test, we defined a dissolution parameter, z, independent of the amount of drug applied and the volume of the dissolution medium. In the dissolution tests of ivermectin, dipyridamole, and phenytoin, the amount applied did not affect the z value. Both small and large applications resulted in similar z values, indicating that the compound consumption for the dissolution test could be reduced.

Here we conducted miniscale dissolution tests using 50 mL of dissolution medium with a 100-mL small vessel and a minipaddle. This system is a scaled-down model of the conventional 1000-mL vessels and paddles. The miniscale dissolution test required one tenth of the dissolution medium compared to current testing methods. In the present study, therefore, the dissolution test can be carried out with 1 mg of the combined compounds. The reduced amount of drug consumption utilized in this system would be advantageous in the early stage of drug discovery.

Table VI. The Predicted F_a and Human Absorption Data of 12 Drugs

	Predicted F_a (%) (mean ± SD)		Human absorption data in the literature		
Drug name	SIF[a]	FaSSIF[b]	Clinical dose (mg)	F_a (%)	References
Danazol	8 ± 1	40 ± 2	100	32[c]	(46)
Dipyridamole	32 ± 5	53 ± 2	50	36[d,e]	(15,20)
Efavirenz	8 ± 0	76 ± 2	1200	67[c]	See text
Exemestane	100 ± 0	100 ± 0	25	72[c]	(47)
Gefitinib	24 ± 1	69 ± 2	250	44[d,e]	See text
Griseofulvin	22 ± 1	23 ± 1	500	43[f]	(40)
Ivermectin	5 ± 0	53 ± 10	12	56[f]	See text
Ketoconazole	6 ± 1	9 ± 2	200	4[e,f]	(21,22)
Ketoprofen	100 ± 0	100 ± 0	25	100[f]	(48)
Nitrendipine	77 ± 10	100 ± 0	20	73[d]	(49)
Phenytoin	100 ± 0	100 ± 0	300	84[c]	(50)
Spironolactone	99 ± 1	100 ± 0	200	100[f]	(51)

[a] Predicted F_a using the dissolution results in SIF.
[b] Predicted F_a using the dissolution results in FaSSIF.
[c] Calculated from the clinical absorption data of a solid dosage form orally administered in the fasted and fed states.
[d] Calculated from the bioavailabilities of a solid dosage form administration in the fasted states and total plasma clearance assuming that hepatic clearance is the only elimination pathway.
[e] Oral absorption data of weak base drugs in subjects with elevated gastric pH ($F_{a,low}$).
[f] Calculated from the clinical absorption data of a solid dosage form and a solution orally administered in the fasted states.

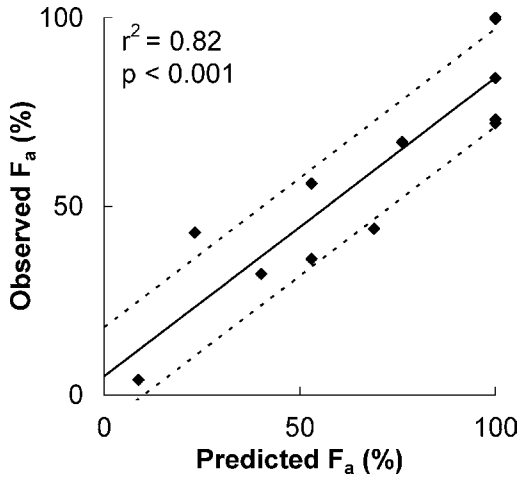

Fig. 6. Correlation between *in vivo* human F_a and predicted F_a using the dissolution results in FaSSIF. Dotted lines signify the standard error between observed and predicted F_a.

The *in vivo* dissolution of poorly water-soluble drugs can depend strongly on fluid pH and bile salts secretion in the GI tract (25,29–31). Thus, considerable care must be taken in the choice of the *in vitro* dissolution medium for predicting oral absorption. In the present study, we compared solubility and dissolution rates in two types of dissolution media: 1) simulated intestinal fluid (SIF, pH 6.5) not including bile salts and 2) fasted-state simulated intestinal fluid (FaSSIF, pH 6.5), a biorelevant medium containing sodium taurocholate and lecithin reported by Galia *et al.* (25).

The saturated solubility of the model drugs was higher in FaSSIF than in SIF. The increase in solubility in FaSSIF could be due to micellar solubilization. On the other hand, the dissolution parameter z decreased in FaSSIF (Table IV). The value of z depends on the diffusion coefficient, diffusion layer thickness, initial particle radius, and density of the drug. The diffusion coefficient has been reported to be reduced by micellar solubilization because diffusivity of a micelle drug complex would be smaller than that of a free drug (32,33). For example, the diffusivity of danazol was almost halved in a bile salt and lecithin micellar solution (19). Because media properties should not affect other parameters, decreased dissolution parameters of these drugs observed in FaSSIF are likely due to the contribution of the decreased diffusion coefficient. These results indicate that not only solubility but also the dissolution parameter are essential to simulate dissolution of BCS class II drugs.

The dissolutions of exemestane and phenytoin were slightly faster in SIF than in FaSSIF in spite of higher solubility in FaSSIF (Fig. 2). Although the reason for this inconsistent result is not clear, decreased diffusion coefficients by incorporation in the micelle may induce these results.

To simulate precisely the oral drug absorption in humans, the P_{eff} values of the human intestine are necessary. However, at the drug discovery stage, it is impossible to obtain the real P_{eff} values in humans for drug candidates. Caco-2 study might be available; however, the permeability to Caco-2 monolayer is not the same as P_{eff} in humans. In addition, in the case of lipophilic drugs, the permeability in Caco-2 study is not stable and might not be accurate because of the nonspecific binding of drugs to experimental apparatus or membrane surface. The use of solubilizers also influences drug permeability (26,34,35).

According to the results of a Caco-2 study, the drugs used in this study were confirmed as highly permeable [P_{app} = (3–10) $\times$ 10^{-5} cm/s]. For these highly permeable compounds, the UWL has been suggested to contribute to the major resistance to intestinal absorption (8,36–38). In addition, the calculated P_{UWL} of ketoprofen (9×10^{-4} cm/s) has been shown to be nearly equal to reported human jejunal permeability (9×10^{-4} cm/s) (39). Because this study aimed to predict the human oral absorption of poorly soluble compounds at the early stage of drug development, the precise F_a prediction, such as a one-on-one prediction, is not entirely necessary. Therefore, we have adopted the calculated *UWL* permeability as the P_{eff} value for high membrane permeable compounds.

Undetectable ivermectin in Caco-2 assays may be due to drug adsorption to the apparatus and the Caco-2 membrane. Because ivermectin is a highly lipophilic compound (Table I), diffusion through the *UWL* is likely to be slower than permeation through the hydrophobic intestinal membrane.

Concerning the simulation of oral absorption, the time course of the absorbed drug was almost the same as that of the total dissolved drug for ivermectin, efavirenz (Figs. 4 and 5A), and other drugs (data not shown). Because the absorption rate reflects the rate of the limiting step, the simulated absorption in this study would be limited by drug dissolution.

The oral absorption of BCS class II drugs is limited by the dissolution rate if the dose to solubility ratio is low (4). In the case of a low ratio, the drug dissolution *in vivo* occurs under sink conditions. On the other hand, if the dose to solubility ratio is high as in high-dose drug administration, the oral absorption is limited not only by the dissolution rate but also by the saturated solubility and dissolution occurs under nonsink conditions. Ivermectin was simulated to dissolve under sink conditions ($C_s \gg X_{d,vivo}(t)/V_{vivo}$, Fig. 4B), and so we expected that the absorption would be limited by the dissolution rate. On the other hand, the C_{ratio} of efavirenz was simulated to increase to 40% within 4 h (Fig. 5B) because the clinical dose of efavirenz is too high (a dose to solubility ratio of 6 L) to be dissolved. We expect that the absorption of efavirenz would be limited by the dissolution rate and solubility. To confirm the rate-limiting steps of both drugs in humans, we have analyzed the clinical data of ivermectin and efavirenz. The limiting steps for absorption of a drug *in vivo* can be deduced from the dose dependency of bioavailability. The amount of drug absorbed would increase dose dependency when the oral absorption is limited by the dissolution rate, whereas the oral absorption would reach a ceiling at the dose when solubility-limited absorption occurs. The absorbed amount of ivermectin has been reported to increase linearly with increasing doses in the range of 6–15 mg in humans, so its oral absorption in humans can be regarded as dissolution rate limited [approval documentation for Stromectol® (ivermectin), NDA no. 050742, 1996, Merck & Co., Inc, Whitehouse Station, NJ, USA]. On the other hand, the oral absorption of efavirenz in the fasted state is considered to reach a ceiling at high doses (1200 mg) because the *rel.* $BA_{fasted/fed}$ [Eq (15)] was 100% at 100 mg but 67% at a high dose (1200 mg) [approval documentation for Sustiva™ (efavirenz), NDA no. 020972,

1998, DuPont Pharmaceuticals Company, Wilmington, DE, USA]. The absorption of efavirenz at a high dose in the fasted state could be limited by the dissolution rate and solubility of the drug. These clinical results indicate that our system can simulate not only dissolution-rate-limited but also solubility-limited absorption of BCS class II drugs.

The predicted amount of fraction absorbed of griseofulvin is two times smaller than the mean observed value. In the clinical study, the fraction absorbed of griseofulvin has been reported to vary in the range of 24–53% (40). Therefore, our system could predict the lower limit (24%) of griseofulvin absorption in humans. At present, the reason for this underestimation is not clear. However, in the case of griseofulvin, *in vitro* dissolution in FaSSIF might not reflect the *in vivo* dissolution because the saturated solubility of griseofulvin in FaSSIF was almost the same as that in SIF. In addition, griseofulvin is possible to be absorbed not only in the small intestine but also in the colon because of its high clinical dose (41). The plausibility of these reasons is now under investigation.

In this study, to establish a rational system that evaluates the potential of drug candidates for oral products in the drug discovery stage, we have used the biorelevant medium and the physiological parameters as the appropriate conditions that simulate the oral absorption of BCS class II drugs. The predicted F_a of the 12 BCS class II drugs significantly correlated with clinical data when the dissolution profiles in FaSSIF were used for the simulation ($r^2 = 0.82$, $p < 0.001$, $n = 12$, Fig. 6), whereas SIF medium gave the lower prediction of F_a than the observed data for most drugs. These results clearly indicate that physiologically based medium is advantageous to determine the dissolution profiles of drugs relevant to *in vivo* dissolution behavior. Finally, the predictability of F_a obtained in this system ($r^2 = 0.82$, RMSE = 16%) would be enough and acceptable to evaluate the absorbability of drug candidates in the drug discovery stage (27). In conclusion, the miniscale dissolution test integrated with a computer simulation system could simulate quantitatively the *in vivo* absorption of structurally diverse BCS class II drugs. The newly developed system would be beneficial to characterize drug absorbability for drug candidate selection.

REFERENCES

1. C. A. Lipinski. Drug-like properties and the causes of poor solubility and poor permeability. *J. Pharmacol. Toxicol. Methods* **44**:235–249 (2000).
2. J. B. Dressman, G. L. Amidon, and D. Fleisher. Absorption potential: estimating the fraction absorbed for orally administered compounds. *J. Pharm. Sci.* **74**:588–589 (1985).
3. R. J. Hintz and K. C. Johnson. The effect of particle size distribution on dissolution rate and oral absorption. *Int. J. Pharm.* **51**:9–17 (1989).
4. L. X. Yu. An integrated model for determining causes of poor oral drug absorption. *Pharm. Res.* **16**:1883–1887 (1999).
5. J. B. Dressman and D. Fleisher. Mixing-tank model for predicting dissolution rate control or oral absorption. *J. Pharm. Sci.* **75**:109–116 (1986).
6. A. A. Noyes and W. R. Whitney. The rate of solution of solid substances in their own solutions. *J. Am. Chem. Soc.* **19**:930–934 (1987).
7. K. Obata, K. Sugano, R. Saitoh, A. Higashida, Y. Nabuchi, M. Machida, and Y. Aso. Prediction of oral drug absorption in humans by theoretical passive absorption model. *Int. J. Pharm.* **293**:183–192 (2005).
8. H. Lennernas. Human intestinal permeability. *J. Pharm. Sci.* **87**:403–410 (1998).
9. J. C. McGowan. Estimates of the Properties of Liquids. *J. Appl. Chem. Biotechnol.* **28**:599–607 (1978).
10. U. Fagerholm, L. Borgstrom, O. Ahrenstedt, and H. Lennernas. The lack of effect of induced net fluid absorption on the *in vivo* permeability of terbutaline in the human jejunum. *J. Drug Target.* **3**:191–200 (1995).
11. R. H. Perry and D. W. Green. *Perry's Chemical Engineers' Platinum Edition*, McGraw-Hill, New York, 1999.
12. J. B. Dressman. Comparison of canine and human gastrointestinal physiology. *Pharm. Res.* **3**:123–131 (1986).
13. R. Lobenberg and G. L. Amidon. Modern bioavailability, bioequivalence and biopharmaceutics classification system. New scientific approaches to international regulatory standards. *Eur. J. Pharm. Biopharm.* **50**:3–12 (2000).
14. J. B. Dressman and C. Reppas. *In vitro–in vivo correlations for lipophilic, poorly water-soluble drugs. Eur. J. Pharm. Sci.* **11**(2):S73–S80 (2000).
15. T. D. Bjornsson and C. Mahony. Clinical pharmacokinetics of dipyridamole. *Thromb. Res. Suppl.* **4**:93–104 (1983).
16. B. Davies and T. Morris. Physiological parameters in laboratory animals and humans. *Pharm. Res.* **10**:1093–1095 (1993).
17. O. Fausa. Duodenal bile acids after a test meal. *Scand. J. Gastroenterol.* **9**:567–570 (1974).
18. A. Tangerman, A. Schaikvan, and E. W. van der Hoek. Analysis of conjugated and unconjugated bile acids in serum and jejunal fluid of normal subjects. *Clin. Chim. Acta.* **159**:123–132 (1986).
19. L. J. Naylor, V. Bakatselou, N. Rodriguez-Hornedo, N. D. Weiner, and J. B. Dressman. Dissolution of steroids in bile salt solutions is modified by the presence of lecithin. *Eur. J. Pharm. Biopharm.* **41**:346–353 (1995).
20. T. L. Russell, R. R. Berardi, J. L. Barnett, T. L. O'Sullivan, J. G. Wagner, and J. B. Dressman. pH-related changes in the absorption of dipyridamole in the elderly. *Pharm. Res.* **11**:136–143 (1994).
21. R. A. Blum, D. T. D'Andrea, B. M. Florentino, J. H. Wilton, D. M. Hilligoss, M. J. Gardner, E. B. Henry, H. Goldstein, and J. J. Schentag. Increased gastric pH and the bioavailability of fluconazole and ketoconazole. *Ann. Intern. Med.* **114**:755–757 (1991).
22. Y. C. Huang, J. L. Colaizzi, R. H. Bierman, R. Woestenborghs, and J. Heykants. Pharmacokinetics and dose proportionality of ketoconazole in normal volunteers. *Antimicrob. Agents Chemother.* **30**:206–210 (1986).
23. L. A. Radesca, M. B. Maurin, S. R. Rabel, and J. R. Moore. Crystalline efavirenz. PCT Patent WO 99 64405 A1 (1999).
24. G. J. Peter, G. A. Stephen, Y. B. Ingvar, and B. Martin. Novel crystalline forms of the anti-cancer compound ZD1839. PCT Patent WO 03 072108 A1 (2003).
25. E. Galia, E. Nicolaides, D. Horter, R. Lobenberg, C. Reppas, and J. B. Dressman. Evaluation of various dissolution media for predicting *in vivo* performance of class I and II drugs. *Pharm. Res.* **15**:698–705 (1998).
26. B. J. Aungst, N. H. Nguyen, J. P. Bulgarelli, and K. Oates-Lenz. The influence of donor and reservoir additives on Caco-2 permeability and secretory transport of HIV protease inhibitors and other lipophilic compounds. *Pharm. Res.* **17**:1175–1180 (2000).
27. N. Parrot and T. Lave. Prediction of intestinal absorption: comparative assessment of GASTROPLUS and IDEA. *Eur. J. Pharm. Sci.* **17**:51–61 (2002).
28. E. Nicolaides, M. Symillides, J. B. Dressman, and C. Reppas. Biorelevant dissolution testing to predict the plasma profile of lipophilic drugs after oral administration. *Pharm. Res.* **18**:380–388 (2001).
29. E. Nicolaides, E. Galia, C. Efthymiopoulos, J. B. Dressman, and C. Reppas. Forecasting the *in vivo* performance of four low solubility drugs from their *in vitro* dissolution data. *Pharm. Res.* **16**:1876–1882 (1999).

30. V. J. Stella, S. Martodihardjo, and V. M. Rao. Aqueous solubility and dissolution rate does not adequately predict *in vivo* performance: a probe utilizing some *N*-acyloxymethyl phenytoin prodrugs. *J. Pharm. Sci.* **88**:775–779 (1999).
31. V. H. Sunesen, B. L. Pedersen, H. G. Kristensen, and A. Mullertz. *In vivo in vitro* correlations for a poorly soluble drug, danazol, using the flow-through dissolution method with biorelevant dissolution media. *Eur. J. Pharm. Sci.* **24**:305–313 (2005).
32. R. J. Braun and E. L. Parrott. Influence of viscosity and solubilization on dissolution rate. *J. Pharm. Sci.* **61**:175–178 (1972).
33. J. R. Crison, V. P. Shah, J. P. Skelly, and G. L. Amidon. Drug dissolution into micellar solutions: development of a convective diffusion model and comparison to the film equilibrium model with application to surfactant-facilitated dissolution of carbamazepine. *J. Pharm. Sci.* **85**:1005–1011 (1996).
34. S. Yamashita, T. Furubayashi, M. Kataoka, T. Sakane, H. Sezaki, and H. Tokuda. Optimized conditions for prediction of intestinal drug permeability using Caco-2 cells. *Eur. J. Pharm. Sci.* **10**:195–204 (2000).
35. Y. Takahashi, H. Kondo, T. Yasuda, T. Watanabe, S. Kobayashi, and S. Yokohama. Common solubilizers to estimate the Caco-2 transport of poorly water-soluble drugs. *Int. J. Pharm.* **246**:85–94 (2002).
36. M. D. Levitt, J. K. Furne, A. Strocchi, B. W. Anderson, and D. G. Levitt. Physiological measurements of luminal stirring in the dog and human small bowel. *J. Clin. Invest.* **86**:1540–1547 (1990).
37. M. D. Levitt, T. Aufderheide, C. A. Fetzer, J. H. Bond, and D. G. Levitt. Use of carbon monoxide to measure luminal stirring in the rat gut. *J. Clin. Invest.* **74**:2056–2064 (1984).
38. D. Winne, H. Gorig, and U. Muller. Closed rat jejunal segment *in situ*: role of pre-epithelial diffusion resistance (unstirred layer) in the absorption process and model analysis. *Naunyn-Schmiedeberg's Arch. Pharmacol.* **335**:204–215 (1987).
39. N. A. Kasim, M. Whitehouse, C. Ramachandran, M. Bermejo, H. Lennernas, A. S. Hussain, H. E. Junginger, S. A. Stavchansky, K. K. Midha, V. P. Shah, and G. L. Amidon. Molecular properties of WHO essential drugs and provisional biopharmaceutical classification. *Mol. Pharm.* **1**:85–96 (2004).
40. W. L. Chiou and S. Riegelman. Absorption characteristics of solid dispersed and micronized griseofulvin in man. *J. Pharm. Sci.* **60**:1376–1380 (1971).
41. A. L. Ungell, S. Nylander, S. Bergstrand, A. Sjoberg, and H. Lennernas. Membrane transport of drugs in different regions of the intestinal tract of the rat. *J. Pharm. Sci.* **87**:360–366 (1998).
42. I. E. Borisevitch and M. Tabak. Electronic absorption and fluorescence spectroscopic studies of dipyridamole: effects of solution composition. *J. Lumin.* **51**:315–322 (1992).
43. K. Box, C. Bevan, J. Comer, A. Hill, R. Allen, and D. Reynolds. High-throughput measurement of pK_a values in a mixed-buffer linear pH gradient system. *Anal. Chem.* **75**:883–892 (2003).
44. I. Legen and A. Kristl. pH and energy dependent transport of ketoprofen across rat jejunum *in vitro*. *Eur. J. Pharm. Biopharm.* **56**:87–94 (2003).
45. H. Wan, A. G. Holmen, Y. Wang, W. Lindberg, M. Englund, M. B. Nagard, and R. A. Thompson. High-throughput screening of pK_a values of pharmaceuticals by pressure-assisted capillary electrophoresis and mass spectrometry. *Rapid Commun. Mass Spectrom.* **17**:2639–2648 (2003).
46. W. N. Charman, M. C. Rogge, A. W. Boddy, and B. M. Berger. Effect of food and a monoglyceride emulsion formulation on danazol bioavailability. *J. Clin. Pharmacol.* **33**:381–386 (1993).
47. M. Valle, E. SalleDi, M. G. Jannuzzo, I. Poggesi, M. Rocchetti, R. Spinelli, and D. Verotta. A predictive model for exemestane pharmacokinetics/pharmacodynamics incorporating the effect of food and formulation. *Br. J. Clin. Pharmacol.* **59**:355–364 (2005).
48. S. Stiegler, M. Birkel, V. Jost, R. Lange, P. W. Lucker, and N. Wetzelsberger. Pharmacokinetics and relative bioavailability after single dose administration of 25 mg ketoprofen solution as compared to tablets. *Methods Find. Exp. Clin. Pharmacol.* **17**:129–134 (1995).
49. G. Mikus, C. Fischer, B. Heuer, C. Langen, and M. Eichelbaum. Application of stable isotope methodology to study the pharmacokinetics, bioavailability and metabolism of nitrendipine after i.v. and p.o. administration. *Br. J. Clin. Pharmacol.* **24**: 561–569 (1987).
50. A. Melander, G. Brante, O. Johansson, T. Lindberg, and E. Wahlin-Boll. Influence of food on the absorption of phenytoin in man. *Eur. J. Clin. Pharmacol.* **15**:269–274 (1979).
51. A. Karim, J. Zagarella, T. C. Hutsell, A. Chao, and B. J. Baltes. Spironolactone. II. Bioavailability. *Clin. Pharmacol. Ther.* **19**: 170–176 (1976).